nature astronomy

Article

https://doi.org/10.1038/s41550-026-02791-z

# A complete set of canonical nucleobases in the carbonaceous asteroid (162173) Ryugu

Received: 8 July 2025

Accepted: 20 January 2026

Published online: 16 March 2026

Check for updates

Toshiki Koga[1] ✉, Yasuhiro Oba[2], Yoshinori Takano[1,3], Hiroshi Naraoka[4], Nanako O. Ogawa[1], Kazunori Sasaki[5], Hajime Sato[5], Toshihiro Yoshimura[1] & Naohiko Ohkouchi[1]

Organic molecules delivered from extraterrestrial materials may have played a key role in supplying building blocks for life on Earth. Here we report all five canonical nucleobases—purines (adenine and guanine) and pyrimidines (cytosine, thymine and uracil)—in samples returned from the C-type asteroid (162173) Ryugu by JAXA's Hayabusa2 mission and compare the results with data from similar extraterrestrial material. Ryugu samples contain nearly equal amounts of purines and pyrimidines, whereas Murchison is enriched in purines and Bennu and Orgueil in pyrimidines. Samples from Ryugu, Bennu and Orgueil, which have a similar mineralogy and elemental composition, show purine-to-pyrimidine ratios negatively correlating with ammonia. These observations indicate that the nucleobases in these samples may have formed via a shared pathway depending on the physicochemical environment of the respective parent bodies. The detection of diverse nucleobases in asteroid and meteorite materials demonstrates their widespread presence throughout the Solar System and reinforces the hypothesis that carbonaceous asteroids contributed to the prebiotic chemical inventory of early Earth.

Nucleic acids and their molecular components (nucleobases) are fundamental biomolecules sustaining life on Earth. The purines adenine and guanine and the pyrimidines cytosine, uracil and thymine constitute the base sequences of DNA and RNA that encode and transmit genetic information[1]. Beyond heredity, nucleotides—nucleobases linked to sugars and phosphate groups—serve as essential energy carriers, such as adenosine triphosphate (ATP)[2], and as key coenzymes, including nicotinamide adenine dinucleotide ($NAD^+$/NADH)[3], highlighting the biochemical indispensability of nucleobases and their derivatives.

In prebiotic chemistry, the 'RNA world' hypothesis[4–6] emphasizes the role of ribonucleic acids as both genetic carriers and catalysts, making nucleobases indispensable for early biochemical systems. The universal reliance of metabolism on adenine-based cofactors and energy currencies further indicates that this molecular architecture reflects ancient chemical constraints[7]. Accordingly, understanding the sources and availability of nucleobases on the early Earth remains a central question in origins-of-life research.

Because of their essential roles in both biochemistry and prebiotic chemistry, nucleobases have become a focus in cosmochemistry and astrobiology. The detection of nucleobases in carbonaceous meteorites[8–10] demonstrates that these molecules can be synthesized abiotically under interstellar ice and aqueous planetary conditions. This implies that the molecular prerequisites for life are not unique to Earth and may emerge as natural products of chemical evolution throughout the Solar System. Nucleobases could have been delivered to the early Earth, potentially contributing to the molecular inventory necessary for life[11]. Furthermore, elucidating the formation mechanisms of extraterrestrial nucleobases helps to constrain the universal

[1]Biogeochemistry Research Center (BGC), Japan Agency for Marine-Earth Science and Technology (JAMSTEC), Yokosuka, Japan. [2]Institute of Low Temperature Science (ILTS), Hokkaido University, Sapporo, Japan. [3]Institute for Advanced Biosciences (IAB), Keio University, Tsuruoka, Japan. [4]Department of Earth and Planetary Sciences, Kyushu University, Fukuoka, Japan. [5]Human Metabolome Technologies Inc. (HMT), Tsuruoka, Japan. ✉e-mail: toshikikoga@jamstec.go.jp

physicochemical conditions under which they can form abiotically[12], thus linking astrochemical processes in interstellar and planetary environments to the chemical evolution that preceded the origin of life.

To accurately assess the nucleobases in extraterrestrial materials, it is essential to analyse samples minimally altered by terrestrial processes. In this context, pristine asteroid samples—those not exposed to Earth's atmosphere—hold high scientific value, as exemplified by the samples collected by the Hayabusa2 mission from the C-type asteroid (162173) Ryugu[13–16]. Initial analyses of Ryugu samples A0106 and C0107, from the first and second touchdown sites, respectively, revealed diverse organic molecules[17–25], including uracil[26].

However, in contrast to the limited detection of uracil in Ryugu[26], a relatively wide variety of nucleobases has been identified in carbonaceous meteorites, including all five canonical nucleobases and non-biological structural isomers[8–10]. A similar diversity has been observed in a sample from the B-type asteroid (101955) Bennu[27], which was collected by the Origins, Spectral Interpretation, Resource Identification, and Security–Regolith Explorer (OSIRIS-REx) mission[28]. The limited amounts of material available from the Ryugu samples for the initial analysis may have prevented a precise characterization of nucleobase distributions, rather than indicating an actual deficiency of nucleobases.

Recent studies have reported variations in nucleobase contents in extraterrestrial materials: pyrimidines are more abundant than purines in the Bennu sample[27], whereas purines are dominant in the Murchison carbonaceous meteorite[10]. Given that Bennu experienced more alkaline and ammonia-rich aqueous alteration than Ryugu[22,27], analysing both purines and pyrimidines in Ryugu samples is crucial for understanding how nucleobase distributions reflect the chemical history and formation processes in different primitive parent bodies. In this study, we report a comprehensive analysis of nucleobases in two Ryugu aggregate samples (A0480 and C0370; Supplementary Fig. 1) using sufficient sample material and optimized analytical techniques. The CI1 (Ivuna-type) Orgueil meteorite was analysed as a comparative reference because of its mineralogical and elemental similarities to the Ryugu samples[29,30].

## Results

The Ryugu A0480 and C0370 samples and the Orgueil meteorite were first subjected to water extraction ($H_2O$ extract), followed by extraction with 6 M hydrochloric acid (HCl extract) (Methods). Following the sequential extraction, we performed nanoscale elemental analysis–isotope-ratio mass spectrometry (nano-EA/IRMS)[31,32] on the extracted residues. The carbon (C) and nitrogen (N) contents and their isotopic compositions in the residues were intermediate between those of the initial bulk[17,26] and the insoluble organic matter[21,33], with consistent trends across both Ryugu and Orgueil samples (Extended Data Fig. 1 and Extended Data Table 1). Mass balance calculations indicate that approximately 30–40% of the total C and N in the Ryugu samples are present as water- and acid-soluble components. These soluble components exhibit broad ranges of relatively heavy C ($\delta^{13}C$ = +25.5‰ to +33.9‰) and N ($\delta^{15}N$ = +45.1‰ to +59.8‰) isotopic compositions that are substantially enriched relative to the terrestrial organic ranges ($\delta^{13}C$ = −35‰ to −10‰ and $\delta^{15}N$ = −10‰ to +20‰)[34], whereas the insoluble organic matter has narrower and lighter isotopic ($\delta^{13}C$ = −18.3‰ to −17.0‰ and $\delta^{15}N$ = +28.2‰ to +29.1‰) signatures (Supplementary Information).

Our high-performance liquid chromatography coupled with electrospray ionization high-resolution mass spectrometry (HPLC/ESI-HRMS) analysis detected chromatographic peaks corresponding to adenine (~14.0 min), hypoxanthine (~5.1 min), guanine (~8.2 min) and xanthine (~4.9 min) in the HCl extracts of the A0480 and C0370 samples, with retention times consistent with those of authentic standards (Fig. 1 and Supplementary Table 1). Most of these purine nucleobases were likewise detected in the $H_2O$ extracts, except for xanthine in A0480 and adenine in C0370. The absence or near absence of corresponding peaks in the procedural blanks indicates that these compounds are indigenous to the samples. Although hypoxanthine and xanthine are not canonical purine nucleobases in DNA or RNA, they are key intermediates in de novo nucleotide biosynthesis. A structural isomer of hypoxanthine (~6.8 min) could not be identified due to the lack of a reference standard, although its presence has been reported in the Murchison meteorite[10] and asteroid Bennu[27] samples. On the basis of proposed formation mechanisms for purine nucleobases in the parent body of the Murchison meteorite[10], this hypoxanthine isomer may correspond to 8-hydroxypurine (7*H*-purin-8-ol). Other purine nucleobases previously reported in meteorites[8–10] and Bennu[27]—including isoguanine, 2-aminopurine, purine, 2,6-diaminopurine and 6,8-diaminopurine—were searched for but not detected.

HPLC/ESI-HRMS analyses using an alternative separation column confirmed the chromatographic peaks of cytosine (~7.5 min), uracil (~11.5 min) and thymine (~16.3 min) in the $H_2O$ and HCl extracts of the A0480 and C0370 samples, with retention times consistent with those of authentic standards (Fig. 2 and Supplementary Table 1). Moreover, 6-methyluracil (~15.2 min), a structural isomer of thymine and a compound rarely reported in biological contexts, was also identified in the Ryugu samples. Owing to the limited amount of material available, only two compounds—guanine and cytosine—in the HCl extract of the C0370 sample were present in sufficient quantities to permit a tandem mass spectrometry analysis (Methods). The resulting fragmentation patterns were consistent with those of the guanine and cytosine standards (Extended Data Figs. 2 and 3). As another approach to support compound identifications in the absence of tandem mass spectrometry, we performed capillary electrophoresis coupled with high-resolution mass spectrometry (CE-HRMS). The CE-HRMS analyses corroborated the presence of purine and pyrimidine nucleobases in the Ryugu samples (Extended Data Figs. 4 and 5). Collectively, these results provide robust evidence for the presence of all five canonical nucleobases—adenine, guanine, cytosine, thymine and uracil—in the Ryugu samples.

Consistent with previous analyses of the A0106 and C0107 samples[26], nicotinic acid (niacin or vitamin $B_3$) and its isomer isonicotinic acid (including four other unidentified isomers) were also detected in the A0480 and C0370 samples (Extended Data Fig. 6). All N-containing heterocycles identified in the Ryugu samples were likewise found in the Orgueil meteorite (Supplementary Fig. 1 and Supplementary Table 2). Beyond N-heterocycles, urea, ethanolamine and several amino acids were detected in the Ryugu samples (Supplementary Information, Extended Data Fig. 7 and Extended Data Table 2).

Table 1 summarizes the concentrations of 15 N-containing heterocyclic compounds, including purine and pyrimidine nucleobases, in the $H_2O$ and HCl extracts of the Ryugu A0480 and C0370 samples as well as the Orgueil meteorite. The total nucleobase concentration ($H_2O$ + HCl) in C0370 (1,577 ± 35 pmol $g^{-1}$) was approximately three times higher than in A0480 (507 ± 21 pmol $g^{-1}$). These values are consistent with previous Ryugu analyses[7], in which uracil concentrations in acid-hydrolysed hot water extracts of A0106 and C0107 samples were 98 ± 38 pmol $g^{-1}$ and 285 ± 57 pmol $g^{-1}$, respectively, which are comparable with the total uracil concentrations in A0480 (86 ± 15 pmol $g^{-1}$) and C0370 (199 ± 11 pmol $g^{-1}$) of this work. The extent of the variation in nucleobase concentration observed between samples from the two touchdown sites falls within the range reported for other hydrophilic organic molecules—including hydroxy acids, amino acids, amines and other water-soluble compounds—in the previous Ryugu analyses of A0106 and C0107[21].

Notable differences were observed in nucleobase distributions between the Ryugu samples and the Orgueil meteorite. In C0370, guanine in the HCl extract was the most abundant nucleobase (445 ± 10 pmol $g^{-1}$), whereas in Orgueil, uracil in the $H_2O$ extract predominated (2,640 ± 47 pmol $g^{-1}$). This contrast is further reflected in their extraction profiles: ~76% of nucleobases in Orgueil were

https://doi.org/10.1038/s41550-026-02791-z

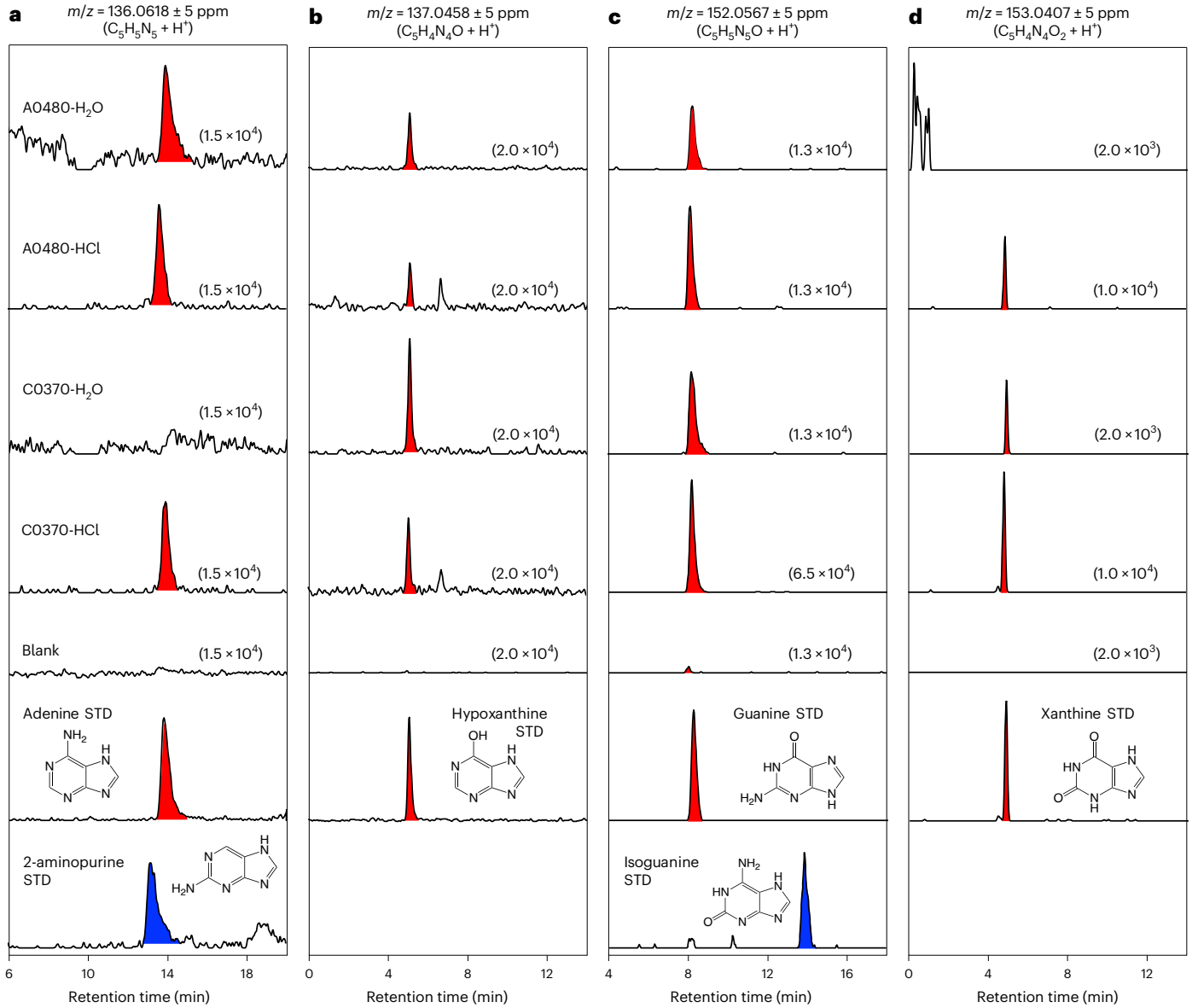


**Fig. 1 | Purine nucleobases detected in the $H_2O$ and HCl extracts of Ryugu A0480 and C0370 samples using HPLC/ESI-HRMS analysis. a**–**d**, Mass chromatograms at the *m/z* of (**a**) 136.0618, (**b**) 137.0458, (**c**) 152.0567 and (**d**) 153.0407, corresponding to the protonated molecular ions of the exact masses for adenine (including its structural isomer 2-aminopurine, $C_5H_5N_5$), hypoxanthine ($C_5H_4N_4O$), guanine (including its structural isomer isoguanine, $C_5H_5N_5O$) and xanthine ($C_5H_4N_4O_2$), respectively. Nucleobases identified with standards are shown in red, and their structural isomers in blue. Data for the procedural blank sample and authentic standards are also shown for comparison. Numbers in parentheses indicate the vertical axis range of each sample chromatogram. STD, standard.

recovered from the $H_2O$ extract, whereas ~60% in A0480 and C0370 were associated with the HCl extracts (Supplementary Information). Differences in nucleobase distributions in extraterrestrial samples can be described in terms of their relative abundances, specifically the purine-to-pyrimidine (Pu/Py) ratios. The Pu/Py ratios of A0480 and C0370 were 1.1 ± 0.2 and 1.2 ± 0.1, respectively, in contrast to 0.099 ± 0.004 in Orgueil, reflecting a pronounced enrichment of pyrimidines—especially uracil—in the meteorite. Given the overall similarity between Ryugu and CI chondrites in terms of elemental, chemical and mineralogical properties[29,30], the marked difference in nucleobase composition is particularly striking.

## Discussion

The detection of structural isomers of nucleobases—an unidentified hypoxanthine isomer (Fig. 1) and 6-methyluracil (Fig. 2)—along with the complex molecular distribution of methylated nicotinic acids (Extended Data Fig. 6 and Supplementary Fig. 1), supports the indigenous origin of all five canonical nucleobases observed in the Ryugu samples and the Orgueil meteorite. Notably, the detection of 6-methyluracil in comparable abundance to thymine indicates that thymine was not the dominant isomer among methylated uracil derivatives generated by chemical processes on Ryugu's parent body. The observed nucleobase distributions in the Ryugu samples (Table 1) deviate from Chargaff's rule[35]—which states that purine and pyrimidine bases occur in a 1:1 ratio in the DNA of all organisms—further supporting the interpretation that the nucleobases identified in both the Ryugu samples and the Orgueil meteorite are of non-biological, extraterrestrial origin.

Figure 3a compares the purine and pyrimidine nucleobase abundances among the Ryugu A0480 and C0370 samples, the Bennu sample[27], the Orgueil meteorite, and the CM2 Murchison

https://doi.org/10.1038/s41550-026-02791-z

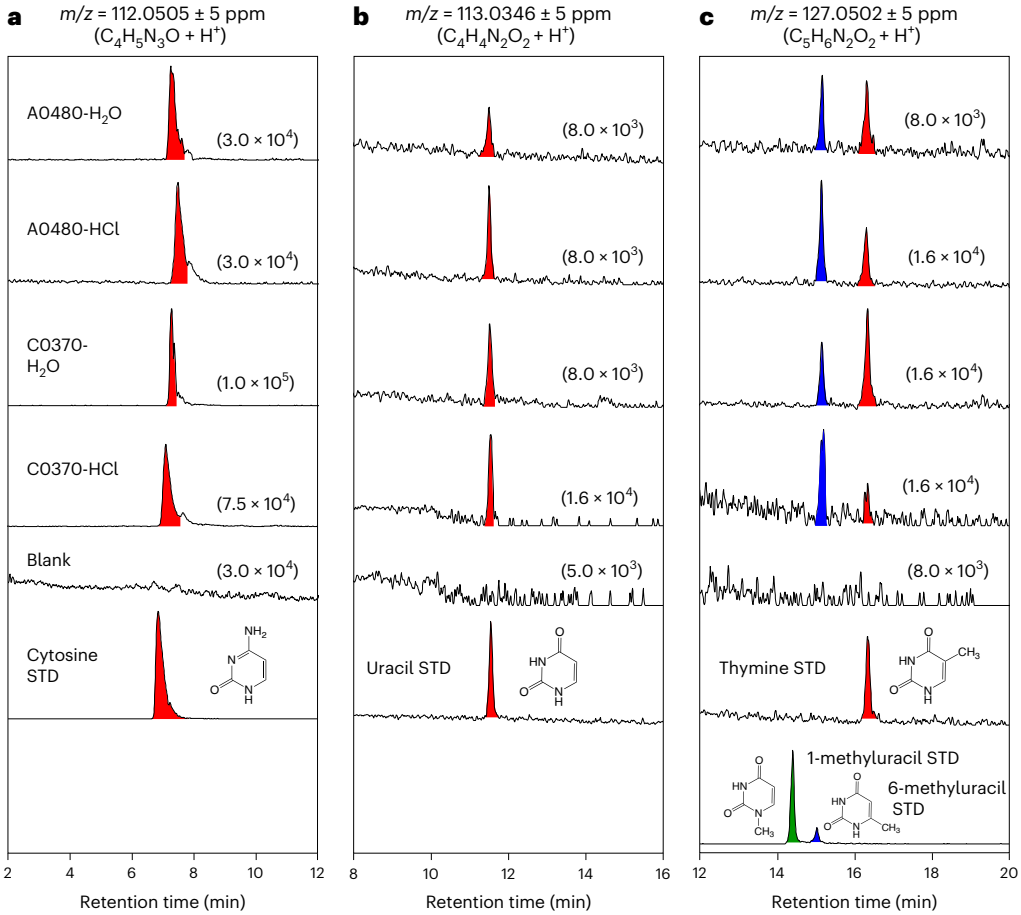


**Fig. 2 | Pyrimidine nucleobases detected in the $H_2O$ and HCl extracts of the Ryugu A0480 and C0370 samples using HPLC/ESI-HRMS analysis.** **a**–**c**, Mass chromatograms at *m/z* of (**a**) 112.0505, (**b**) 113.0346, and (**c**) 127.0502, corresponding to the protonated molecular ions of the exact masses for cytosine ($C_4H_5N_3O$), uracil ($C_4H_4N_2O_2$) and thymine, including its structural isomers 1-methyluracil and 6-methyluracil ($C_5H_6N_2O_2$), respectively. Data for the procedural blank sample and authentic standards are also shown for comparison. Nucleobases identified with standards are shown in red, and their structural isomers in blue and green. Numbers in parentheses indicate the vertical axis range in each sample chromatogram.

meteorite[10]. The total nucleobase concentration in the Ryugu C0370 sample (1,577 ± 35 pmol $g^{-1}$) was less than half that in the Bennu sample (3,404 ± 256 pmol $g^{-1}$, 1$\sigma$)[27]. This difference may reflect the N-rich composition of Bennu, as indicated by the diverse molecular distribution of its soluble organic matter—including amino acids, amines, carboxylic acids and N-heterocycles[27]—in contrast to the sulfur-rich chemistry observed in the Ryugu samples[17,18]. Uracil was the most abundant nucleobase detected in the Bennu sample (0.90 ± 0.06 nmol $g^{-1}$)[27], as it was in the nucleobase distribution observed in the Orgueil meteorite analysed in this study (Table 1). The Orgueil meteorite sample contains the highest total abundance of pyrimidine nucleobases among the four extraterrestrial samples (Fig. 3a). By contrast, the CM2 Murchison meteorite contained higher concentrations of purines (8,861 ± 690 pmol $g^{-1}$, 1$\sigma$) than pyrimidines (2,636 ± 49 pmol $g^{-1}$, 1$\sigma$), indicating a markedly different organic chemistry in the parent body of the CM-type carbonaceous chondrites. This purine dominance may reflect the predominance of hydrogen cyanide (HCN) polymerization-type reactions[36], which are known to efficiently generate purine nucleobases under prebiotic conditions[12]. These substantial differences in nucleobase abundances and compositions among extraterrestrial samples probably reflect the diverse evolutionary histories and chemical conditions of their respective parent bodies, as has also been observed for amino acids[17,19,20,27,37].

Based on comparative analyses of the Ryugu, Bennu, Orgueil and Murchison samples, we propose that the Pu/Py ratio may serve as a useful indicator for distinguishing differences in nucleobase chemistry among carbonaceous asteroids and meteorites (Fig. 3b). The Pu/Py ratios of the Ryugu samples (~1.1–1.2) are higher than those of Bennu (~0.55)[27] and the Orgueil meteorite (~0.10) but substantially lower than that of Murchison (~3.4)[10]. In contrast to the high Pu/Py ratio in Murchison, the lower Pu/Py ratios in the Ryugu, Bennu and Orgueil samples indicate alternative synthetic pathways, with only a minor role for HCN polymerization. A strong correlation ($R^2$ = 0.89) between Pu/Py ratios and ammonia concentrations[22,27] in the Ryugu, Bennu and Orgueil samples (Fig. 3c) provides valuable insight into nucleobase synthesis on their parent bodies. This correlation implies that ammonia availability may have been a key factor driving similar nucleobase formation pathways in these distinct environments.

Only a few laboratory experiments have demonstrated the simultaneous formation of purine and pyrimidine nucleobases under plausible astrochemical or prebiotic conditions. Photochemical reactions of interstellar ice analogues[38], which simulate the chemical evolution in molecular clouds, produced nucleobases with lower Pu/Py ratios (~0.034; Fig. 3b) and dominated by uracil. This indicates that the abundant uracil in the Bennu and Orgueil samples may have been inherited from cold molecular cloud signatures[27]. Furthermore, the proton irradiation of formamide ($HCONH_2$) with meteorite powders as catalysts[39] yielded Pu/Py ratios ranging from 0.38 to 1.3 (Fig. 3b). Although the detection of formamide has not been reported to date in any meteorite or asteroid samples, its detection

https://doi.org/10.1038/s41550-026-02791-z

**Table 1 | Blank-subtracted abundances (in pmol g$^{-1}$) of nucleobases and N-heterocycles detected in the Ryugu A0480 and C0370 samples and Orgueil meteorite using HPLC/ESI-HRMS**

| Abundance | A0480 | | | C0370 | | | Orgueil | | |
|---|---|---|---|---|---|---|---|---|---|
| (pmol g$^{-1}$) | $H_2O$ | HCl | Total | $H_2O$ | HCl | Total | $H_2O$ | HCl | Total |
| **Canonical nucleobases** | | | | | | | | | |
| Uracil | 26±3 (3) | 60±14 (3) | 86±15 | 100±5 (3) | 99±10 (4) | 199±11 | 2,640±47 (2) | 520±46 (2) | 3,160±66 |
| Thymine | 24±4 (3) | 34±2 (2) | 58±5 | 79±11 (3) | 55±10 (4) | 134±14 | 218±7 (2) | 38±2 (2) | 256±7 |
| Cytosine | 6.8±0.5 (3) | 14±4 (3) | 21±4 | 185±24 (4) | 122±2 (2) | 307±24 | n.d. | 23±3 (2) | 23±3 |
| Adenine | 46±11 (2) | 36±2 (2) | 83±11 | n.d. | 49±3 (2) | 49±3 | n.d. | 34.7±3.8 (2) | 35±4 |
| Guanine | 49±2 (2) | 56±2 (2) | 106±3 | 114±2 (2) | 445±10 (2) | 558±10 | 18.7±0.2 (2) | 222±9 (2) | 240±9 |
| **Other purines and pyrimidines** | | | | | | | | | |
| Hypoxanthine | 27±2 (2) | 17±1 (2) | 44±2 | 82.4±0.4 (2) | 40.3±0.4 (2) | 123±1 | n.d. | 17.9±0.4 (2) | 17.9±0.4 |
| Xanthine | n.d. | 36±2 (2) | 36±2 | 11±2 (2) | 108±9 (2) | 120±9 | n.d. | 77±1 (2) | 77±1 |
| 1-Methyluracil | n.d. | n.d. | n.d. | n.d. | n.d. | n.d. | 72±1 (2) | 10±3 (2) | 82±3 |
| 6-Methyluracil | 22±2 (3) | 51±7 (2) | 73±7 | 43±3 (3) | 45±8 (4) | 88±16 | 153±2 (2) | 56±3 (2) | 209±3 |
| **Other N-heterocycles** | | | | | | | | | |
| Nicotinic acid | 1201±60 (2) | 183±18 (2) | 1,385±63 | n.d. | 533±11 (2) | 533±11 | 2,830±41 (2) | 3,831±338 (2) | 6,662±341 |
| Isonicotinic acid | 164±15 (4) | 29±5 (3) | 193±16 | 287±19 (4) | 134±4 (2) | 420±20 | 862±9 (2) | 749±80 (2) | 1,611±81 |
| 2-Methylnicotinic acid | 25±8 (4) | 12±5 (3) | 38±9 | 46±9 (4) | 32±1 (2) | 77±9 | 778±6 (2) | 411±23 (2) | 1,189±24 |
| 4-Methylnicotinic acid | 131±6 (2) | 14±5 (2) | 145±7 | 176±20 (4) | 50±6 (2) | 226±21 | 192±6 (2) | 163±14 (2) | 355±15 |
| 5-Methylnicotinic acid | 32±9 (2) | 29±1 (2) | 61±9 | 80±4 (4) | 97±6 (2) | 177±7 | 415±3 (2) | 438±40 (2) | 853±40 |
| 6-Methylnicotinic acid | 68±6 (2) | 47±8 (3) | 115±10 | 163±23 (4) | 235±6 (2) | 398±24 | 1013±9 (2) | 839±66 (2) | 1852±66 |
| **Sum of all purines** (pmol g$^{-1}$) | 123±11 | 146±3 | 269±12 | 208±3 | 642±14 | 849±14 | 18.7±0.2 | 351±9 | 370±9 |
| **Sum of all pyrimidines** (pmol g$^{-1}$) | 79±6 | 159±16 | 238±17 | 406±27 | 321±16 | 727±32 | 3,083±48 | 646±47 | 3,729±67 |
| **Sum of all nucleobases** (pmol g$^{-1}$) | 202±13 | 305±17 | 507±21 | 614±27 | 963±21 | 1,577±35 | 3,102±48 | 997±48 | 4,099±67 |
| (% of HCl to total) | (40±3%) | (60±4%) | | (39±2%) | (61±2%) | | (76±2%) | (24±1%) | |
| **Sum of all N-heterocycles** (pmol g$^{-1}$) | 1,823±65 | 620±27 | 2,443±70 | 1,365±47 | 2,044±26 | 3,409±55 | 9,191±65 | 7,429±360 | 16,620±366 |
| **Ratio** (purines/pyrimidines) | 1.6±0.2 | 0.9±0.1 | 1.1±0.1 | 0.51±0.04 | 2.0±0.1 | 1.2±0.1 | 0.0061±0.0001 | 0.54±0.04 | 0.099±0.003 |

Water (25 °C for 15 min in triplicate) and HCl extracts (110 °C for 12 h) of the Ryugu aggregate samples (A0480, 11.9 mg and C0370, 8.3 mg) and the CI1 Orgueil meteorite (30.6 mg) were analysed. Compounds were identified using authentic standards. Uncertainties represent standard errors ($\delta x = \sigma_x \times (n)^{-1/2}$) based on two to four replicate measurements. Uncertainties in the total sums and purine-to-pyrimidine ratios were calculated by propagating the standard errors of the individual concentrations of nucleobases and other N-heterocycles. n.d., not detected (below the detection limit).

in interstellar clouds[40] and comets[41] implies its incorporation into their parent bodies. Given that urea ($NH_2CONH_2$)—the most abundant compound identified in this study (Extended Data Table 2)—structurally resembles formamide, nucleobase synthesis in asteroidal materials may plausibly occur from small N-containing molecules via high-energy irradiation, such as γ-rays associated with the decay of short-lived radionuclides[26], like Al. Such high-energy irradiation has been experimentally demonstrated to induce the formation of amino acids[42] and sugars[43], supporting its potential role in nucleobase formation. Clarifying the formation pathways of purine and pyrimidine under conditions simulating interstellar ices and the effects of high-energy irradiation on N-containing molecules will provide key insights into the evolution of extraterrestrial nucleobases in early Solar System environments.

The influence of ammonia concentration on purine and pyrimidine formation has not yet been experimentally investigated. Conceptually, the Pu/Py ratios may depend on the relative abundances of CHO-containing molecules, N-containing molecules and cyanides within a single reaction system (Extended Data Fig. 8). For example, uracil can form through reactions between malic acid ($C_4H_6O_5$) and urea[44], whereas guanine can be synthesized from HCN and urea[36]. The detection of malic acid[21] and urea (Extended Data Fig. 7a; ref. 21) in Ryugu extracts supports the plausibility of such pathways. We, therefore, hypothesize that variations in ammonia availability—delivered via accreted ices from an outer Solar System reservoir—combined with differences in reactant abundances, modulated nucleobase synthesis on the parent bodies of Ryugu, Bennu and Orgueil. These factors ultimately resulted in the Pu/Py ratios observed in their samples (Extended Data Fig. 8).

An analysis of pristine nucleobase distributions and their isotopic compositions in other carbonaceous meteorites would offer critical insights into the origins of these compounds and the astrochemical processes involving N-containing molecules[27,45,46]. The universal detection of all five canonical nucleobases in samples from the carbonaceous asteroids Ryugu and Bennu highlights the potential contribution of these exogenous molecules[11,47] to the organic inventory that supported prebiotic molecular evolution and ultimately enabled the emergence of RNA and DNA on the early Earth.

https://doi.org/10.1038/s41550-026-02791-z

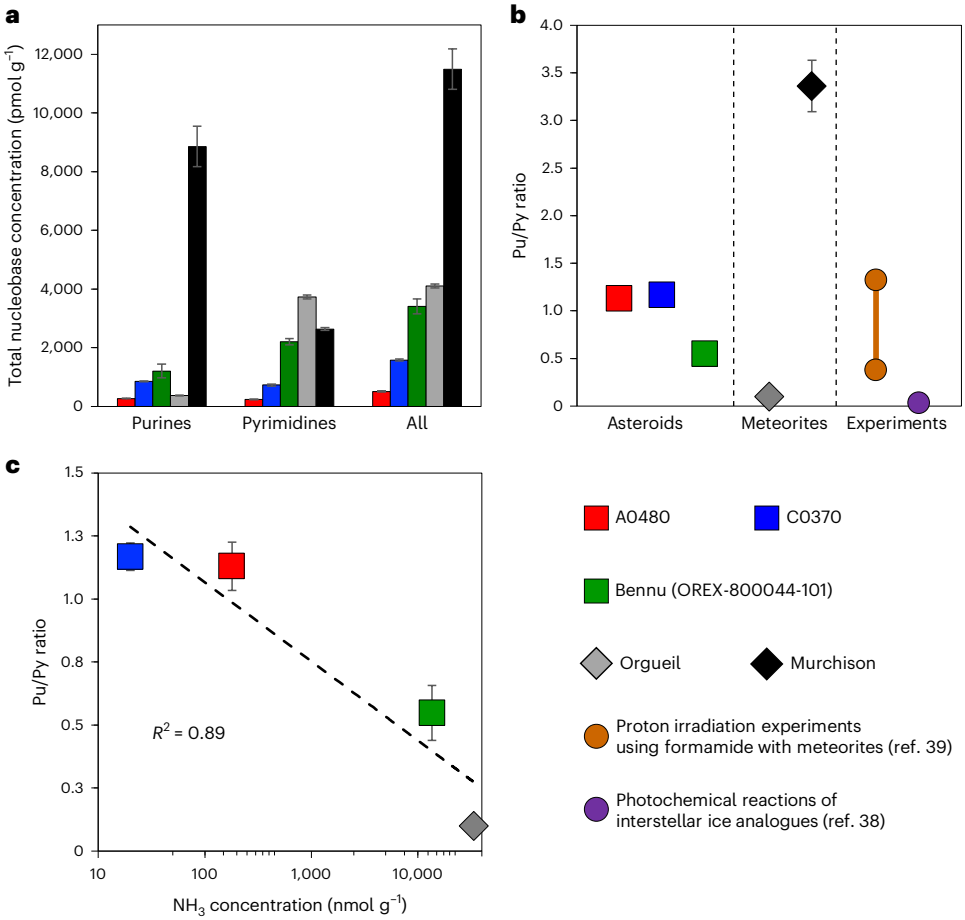


**Fig. 3 | Nucleobase concentrations and abundance ratios of purine and pyrimidine nucleobases in extracts from Ryugu, Bennu and selected carbonaceous meteorites. a**, Comparison of the total concentrations ($H_2O$ + HCl; Table 1) of purine, pyrimidine and all nucleobases in extracts from Ryugu A0480 (red), Ryugu C0370 (blue), Bennu (OREX-800044-101[27]; green), the Orgueil CI meteorite (grey) and the Murchison meteorite[10] (black). Error bars represent propagated standard errors of individual nucleobase concentrations (Table 1). **b**, Purine-to-pyrimidine (Pu/Py) ratios (Table 1) for the same samples. Error bars represent propagated standard errors of individual nucleobase concentrations (Table 1). The ratios for the Orgueil (grey) and Murchison (black) meteorites illustrate distinct differences in nucleobase chemistry among meteorite samples. The brown data points represent the range of relative abundances observed in proton irradiation experiments using formamide with different meteorite powders as catalysts[39]. The purple data point represents the abundance ratio obtained from photochemical reactions of interstellar ice analogues[38]. **c**, The observed correlation ($R^2$ = 0.89) between the Pu/Py ratios (Table 1) and free ammonia concentrations (log scale) in extracts from Ryugu A0480 (red), Ryugu C0370 (blue), Bennu (green) and Orgueil (grey). Error bars represent propagated standard errors of individual nucleobase concentrations (Table 1). Note that ammonia concentrations were determined from hot water extracts from different aggregate samples—A0106 and C0107 for Ryugu[22] and OREX-803001-0 for Bennu[27]—than those used for the nucleobase analyses.

## Methods

### Extraction and purification of organic molecules from samples

The Ryugu A0480 (11.9 mg) and C0370 (8.3 mg) aggregate samples were allocated through the Third Announcement of Opportunity (AO3) by the Japan Aerospace Exploration Agency (JAXA) (Supplementary Fig. 1a). Further descriptions of the Ryugu samples are available in the Ryugu AO database ('Data availability'). Microscope images and near-infrared reflectance spectra (2.0–4.0 µm) (Supplementary Fig. 1) were obtained using the MicrOmega hyperspectral microscope in the clean chamber of the JAXA curation facility before AO3 sample selection, which captured the freshest state of the materials[14,15]. These Ryugu aggregate samples are rich in organic matter[14,15,17,21], and some relevant functional groups (–OH, –NH and –CH) were observed in a non-destructive spectroscopic analysis (Supplementary Data Fig. 1b,c). The data acquisition procedure is available elsewhere[48]. The CI1 Orgueil meteorite (30.6 mg; from the Natural History Museum of Denmark)[21,26] was also analysed as a suitable reference due to its mineralogical and elemental similarities to the Ryugu samples[29,30]. Procedural blanks using baked sea sand (14.4 mg, FUJIFILM Wako Pure Chemical Corporation; 30–50 mesh) and baked serpentine (8.8 mg; 500 °C for 3 h) were prepared following the same protocol as the Ryugu samples and used to assess background signals.

All extraction and purification procedures were conducted on an ISO Class 5 clean bench within an ISO Class 6 clean room at Kyushu University. Each sample was suspended in ultrapure water and transferred to a 1.5 ml polytetrafluoroethylene (PTFE) tube using a glass Pasteur pipette. A total of 550 µl of ultrapure water was used to complete the transfer from the sapphire dish to the PTFE tube. Organic molecules were extracted at 25 °C with 15 min of ultrasonication. After centrifugation for 10 min at 10,000 rpm (equivalent to 14,093*g*), the supernatant was collected in a glass ampoule. The residue was rinsed with 200 µl of ultrapure water, and the rinse was combined with the supernatant to yield approximately ~640 µl in total, designated as the '$H_2O$ extract'. Altogether, 80% of the combined $H_2O$ extracts from the A0480 and C0370 samples were freeze-dried under reduced pressure for subsequent analysis.

The residues extracted from the Ryugu samples were suspended in 600 µl of 6 M HCl and then transferred to glass ampoules using glass Pasteur pipettes. After purging the headspace with dry $N_2$ gas, the ampoules were flame-sealed and heated at 110 °C for 12 h. The HCl

extraction procedure (temperature and duration) was identical to that previously applied to the Bennu sample[27]; however, in the present study, a preliminary water-based ultrasonic extraction at room temperature was performed to selectively isolate molecules that might otherwise be decomposed during acid treatment. Following the acid extraction, the supernatant and sample residues were transferred back into the same PTFE tubes used for the initial water extraction, using glass Pasteur pipettes. After centrifugation for 10 min at 10,000 rpm, the supernatant was collected into a glass ampoule. The residues were washed twice with 200 µl of ultrapure water, and the rinses were combined with the supernatant, designated as the 'HCl extract'. Secondary minerals (for example, carbonates and phyllosilicates)[22,29,30,49] also dissolved during the acid extraction and contributed to the composition of the HCl extract. The entirety of the combined HCl extracts from the A0480 and C0370 samples were freeze-dried under reduced pressure.

The freeze-dried $H_2O$ and HCl extracts were redissolved in 0.5 ml of 0.1 M HCl for desalting using an improved cation-exchange chromatography method[10]. A 0.5-ml aliquot of AG 50W-X8 cation-exchange resin (Bio-Rad Laboratories; analytical grade, 200–400 mesh, hydrogen form) was packed into a glass Pasteur pipette and preconditioned sequentially with 1.5 ml of 1 M HCl, ultrapure water, 1 M NaOH, ultrapure water, 1 M HCl and ultrapure water. The extract solution was then loaded onto the column. The resins were rinsed with 2.5 ml of ultrapure water to recover acidic, neutral and weakly basic compounds (designated as the '$H_2O$ fraction'). Subsequently, 2.5 ml of 10% $NH_4OH$ was applied to elute basic compounds, including most nucleobases (designated as the '$NH_4OH$ fraction'). As a result, four fractions ($H_2O$–$H_2O$, $H_2O$–$NH_4OH$, HCl–$H_2O$, and HCl–$NH_4OH$) were obtained from the Ryugu A0480 and C0370 samples. Despite the prewashing of the cation-exchange chromatography resin, trace amounts of N-containing molecules were detected in the $NH_4OH$ fractions of the procedural blank. These fractions were freeze-dried and reconstituted in 50–100 µl of ultrapure water for subsequent analyses. A fragment of the Orgueil CI meteorite (30.6 mg, purchased from a meteorite trading company) was extracted using the same protocol with ultrapure water and 6 M HCl. Note that the $H_2O$ extract of the Orgueil meteorite was not subjected to cation-exchange chromatography.

### Carbon and nitrogen contents and the isotopic compositions of the extracted residues

The elemental abundances of carbon (C, wt%) and nitrogen (N, wt%) and their isotopic compositions ($\delta^{13}C$ and $\delta^{15}N$, ‰ versus the international standards) in the residues extracted from the A0480, C0370 and the Orgueil meteorite were measured using an ultrasensitive nano-EA/IRMS system (Flash EA1112 elemental analyser/Conflo III interface/Delta Plus XP isotope-ratio mass spectrometer, Thermo Finnigan, Bremen)[31,32]. The masses of the analysed samples were 0.063 mg (A0480), 0.097 mg (C0370) and 0.125 mg (Orgueil). Each residue was loaded into precleaned smooth-wall Sn capsules (Lüdi Swiss AG), whose C and N blanks had been previously evaluated[32]. Isotopic compositions are expressed in conventional δ notation relative to the Vienna Peedee Belemnite for carbon and atmospheric air for nitrogen (denoted as 'standard'), defined as:

$$\delta \equiv 10^3 (R_{\mathrm{sample}}/R_{\mathrm{standard}} - 1)\,(‰), \quad (1)$$

where $R$ represents the $^{13}C/^{12}C$ or $^{15}N/^{14}N$ ratio of the sample ($R_{\mathrm{sample}}$) or the standard ($R_{\mathrm{standard}}$). Calibration was performed using an international and three inter-laboratory standards—L-glutamic acid (USGS-41), L-tyrosine, L-alanine and nickel octaethylporphyrin—spanning $\delta^{13}C$ values from −34.2‰ to +37.4‰ and $\delta^{15}N$ values from +0.86‰ to +47.6‰. The isotope and elemental analyses were calibrated using standards spanning 1.5–27.1 µg (C) and 0.19–3.51 µg (N). The analytical uncertainties, determined from replicate analyses of the L-tyrosine standard, were ±0.27‰ (1$\sigma$, $n$ = 8) for $\delta^{13}C$ and ±0.50‰ (1$\sigma$, $n$ = 9) for $\delta^{15}N$.

### Analysis of nucleobases and other N-containing molecules

The $H_2O$ and HCl extracts derived from the Ryugu and Orgueil samples, alongside procedural blanks and authentic reference compounds, were analysed using a high-resolution online HPLC/ESI-HRMS system[9,10,26,27]. The instrumentation consisted of an UltiMate 3000 HPLC coupled to a mass spectrometer (Q Exactive Plus Hybrid Quadrupole-Orbitrap, Thermo Fisher Scientific), operated at a mass resolution of 140,000 at $m/z$ = 200. A reversed-phase column was maintained at 40 °C for chromatographic separation.

Purine nucleobases were quantified using an isocratic elution programme with a pentafluorophenyl column (1.0 mm × 250 mm, 3-µm particle size; InertSustain, GL Sciences). The mobile phase consisted of 90% water (solvent A) and 10% acetonitrile containing 0.1% (by volume) formic acid (solvent B), delivered at a flow rate of 50 µl $min^{-1}$ for 20 min. For the pyrimidine nucleobase analysis, a column (2.1 mm × 150 mm, 3-µm particle size; HyperCarb, Thermo Fisher Scientific) was used with a linear gradient of solvent A (water plus 0.1% formic acid) and solvent B (acetonitrile plus 0.1% formic acid), progressing from 99:1 at 0 min to 70:30 at 20 min, at a flow rate of 200 µl $min^{-1}$.

The eluent was introduced into a HESI-II ion source (Thermo Fisher Scientific), operated at 280 °C for desolvation. The spray voltage and capillary temperature were set to 3.5 kV and 295 °C, respectively. Full-scan mass spectra were collected in positive ion mode across $m/z$ ranges of 111–155 or 50–500 with mass accuracies better than 5 ppm. Mass calibration was occasionally performed using known ions, including protonated tyrosine ($m/z$ = 182.08117), *tert*-butylamine ($m/z$ = 74.09643) and its fragment ion ($m/z$ = 57.06988), with an acetonitrile dimer ($m/z$ = 83.06037) serving as the lock mass.

For confident identification of guanine and cytosine in the HCl–$NH_4OH$ fraction of the Ryugu C0370 sample, tandem mass spectrometry analyses were performed under the same ionization conditions as the full-scan analyses. The target positive ions were isolated using a quadrupole with a 0.4 atomic mass unit for the isolation window and fragmented by high-energy collisions with $N_2$ gas. The resulting product ions were analysed using a mass spectrometer (Orbitrap) at a resolution of 140,000 at $m/z$ = 200.

To cross-validate the detailed analysis of organic molecules in the Ryugu extracts, CE-HRMS was employed, as previously described[21,26,50]. Briefly, the CE-HRMS measurements were conducted with a capillary electrophoresis system (Agilent 7100, Agilent Technologies) coupled to a mass spectrometer (Q Exactive Plus, Thermo Fisher Scientific), an isocratic HPLC pump (Agilent 1260, Agilent Technologies), an adapter kit (G1603A CE-MS, Agilent Technologies) and a CE-ESI-MS sprayer kit (G1607A, Agilent Technologies). The CE and MS components were interfaced using a fused silica capillary (80 cm total length × 50 µm inner diameter), with a cation buffer solution (H3301-1001, HMT) serving as the electrophoretic electrolyte. Spectral data were acquired in positive ion mode over an $m/z$ range of 60–900 at a resolution of 140,000 at $m/z$ = 200.

## Data availability

Source data for Supplementary Fig. 2 is provided as Supplementary Data 1. The sample properties of the Ryugu A0480 and C0370 aggregate samples were obtained from the Ryugu Sample Database System (A0480: https://darts.isas.jaxa.jp/app/curation/ryugu/allDescription.php?sample_id=2626; C0370: https://darts.isas.jaxa.jp/app/curation/ryugu/allDescription.php?sample_id=2634). Source data are provided with this paper. All other raw data supporting the findings of this study are available from the corresponding author upon reasonable request.

## References

1. Minchin, S. & Lodge, J. Understanding biochemistry: structure and function of nucleic acids. *Essays Biochem.* **63**, 433–456 (2019).

2. Pinna, S. et al. A prebiotic basis for ATP as the universal energy currency. *PLoS Biol.* **20**, e3001437 (2022).
3. Goldman, A. D. & Kacar, B. Cofactors are remnants of life's origin and early evolution. *J. Mol. Evol.* **89**, 127–133 (2021).
4. Kirschning, A. Coenzymes and their role in the evolution of life. *Angew. Chem. Int. Ed.* **60**, 6242–6269 (2021).
5. Joyce, G. F. RNA evolution and the origins of life. *Nature* **338**, 217–224 (1989).
6. Dworkin, J. P., Lazcano, A. & Miller, S. L. The roads to and from the RNA world. *J. Theor. Biol.* **222**, 127–134 (2003).
7. Orgel, L. E. Prebiotic chemistry and the origin of the RNA world. *Crit. Rev. Biochem. Mol. Biol.* **39**, 99–123 (2004).
8. Callahan, M. P. et al. Carbonaceous meteorites contain a wide range of extraterrestrial nucleobases. *Proc. Natl Acad. Sci. USA* **108**, 13995–13998 (2011).
9. Oba, Y. et al. Identifying the wide diversity of extraterrestrial purine and pyrimidine nucleobases in carbonaceous meteorites. *Nat. Commun.* **13**, 2008 (2022).
10. Koga, T., Takano, Y., Oba, Y., Naraoka, H. & Ohkouchi, N. Abundant extraterrestrial purine nucleobases in the Murchison meteorite: implications for a unified mechanism for purine synthesis in carbonaceous chondrite parent bodies. *Geochim. Cosmochim. Acta* **365**, 253–265 (2024).
11. Chyba, C. & Sagan, C. Endogenous production, exogenous delivery and impact-shock synthesis of organic molecules: an inventory for the origins of life. *Nature* **355**, 125–132 (1992).
12. Oró, J. & Kimball, A. P. Synthesis of purines under possible primitive Earth conditions. I. Adenine from hydrogen cyanide. *Arch. Biochem. Biophys.* **94**, 217–224 (1961).
13. Tachibana, S. et al. Pebbles and sands on asteroid (162173) Ryugu: in situ observation and returned particles from two landing sites. *Science* **375**, 1011–1016 (2022).
14. Yada, T. et al. Preliminary analysis of the Hayabusa2 samples returned from C-type asteroid Ryugu. *Nat. Astron.* **6**, 214–220 (2022).
15. Pilorget, C. et al. First compositional analysis of Ryugu samples by the MicrOmega hyperspectral microscope. *Nat. Astron.* **6**, 221–225 (2022).
16. Herd, C. Analyzing asteroid Ryugu. *Science* **379**, 784–785 (2023).
17. Naraoka, H. et al. Soluble organic molecules in samples of the carbonaceous asteroid (162173) Ryugu. *Science* **379**, eabn9033 (2023).
18. Schmitt-Kopplin, P. et al. Soluble organic matter molecular atlas of Ryugu reveals cold hydrothermalism on C-type asteroid parent body. *Nat. Commun.* **14**, 6525 (2023).
19. Parker, E. T. et al. Extraterrestrial amino acids and amines identified in asteroid Ryugu samples returned by the Hayabusa2 mission. *Geochim. Cosmochim. Acta* **347**, 42–57 (2023).
20. Furusho, A. et al. Enantioselective three-dimensional high-performance liquid chromatographic determination of amino acids in the Hayabusa2 returned samples from the asteroid Ryugu. *J. Chromatogr. Open* **5**, 100134 (2024).
21. Takano, Y. et al. Primordial aqueous alteration recorded in water-soluble organic molecules from the carbonaceous asteroid (162173) Ryugu. *Nat. Commun.* **15**, 5708 (2024).
22. Yoshimura, T. et al. Chemical evolution of primordial salts and organic sulfur molecules in the asteroid (162173) Ryugu. *Nat. Commun.* **14**, 5284 (2023).
23. Aponte, J. C. et al. PAHs, hydrocarbons, and dimethylsulfides in asteroid Ryugu samples A0106 and C0107 and the Orgueil (CI1) meteorite. *Earth Planets Space* **75**, 28 (2023).
24. Zeichner, S. S. et al. Polycyclic aromatic hydrocarbons in samples of Ryugu formed in the interstellar medium. *Science* **382**, 1411–1416 (2023).
25. Hashiguchi, M. et al. The spatial distribution of soluble organic matter and their relationship to minerals in the asteroid (162173) Ryugu. *Earth Planets Space* **75**, 73 (2023).
26. Oba, Y. et al. Uracil in the carbonaceous asteroid (162173) Ryugu. *Nat. Commun.* **14**, 1292 (2023).
27. Glavin, D. P. et al. Abundant ammonia and nitrogen-rich soluble organic matter in samples from asteroid (101955) Bennu. *Nat. Astron.* **9**, 199–210 (2025).
28. Lauretta, D. S. et al. Asteroid (101955) Bennu in the laboratory: properties of the sample collected by OSIRIS-REx. *Meteorit. Planet. Sci.* **59**, 2453–2486 (2024).
29. Yokoyama, T. et al. Samples returned from the asteroid Ryugu are similar to Ivuna-type carbonaceous meteorites. *Science* **379**, eabn7850 (2023).
30. Nakamura, T. et al. Formation and evolution of carbonaceous asteroid Ryugu: direct evidence from returned samples. *Science* **379**, eabn8671 (2023).
31. Ogawa, N. O. et al. in *Earth, Life, and Isotopes* (eds Keisuke, K. et al.) 339–353 (Kyoto Univ. Press, 2010).
32. Koga, T. et al. Compound-specific carbon and nitrogen isotopic analyses of underivatized pyrimidine and purine nucleobases. *ACS Earth Space Chem.* **9**, 424–432 (2025).
33. Alexander, C. M. O'.D., Fogel, M., Yabuta, H. & Cody, G. D. The origin and evolution of chondrites recorded in the elemental and isotopic compositions of their macromolecular organic matter. *Geochim. Cosmochim. Acta* **71**, 4380–4403 (2007).
34. Hoefs, J. *Stable Isotope Geochemistry* (Springer-Verlag, 2009).
35. Chargaff, E. Chemical specificity of nucleic acids and mechanism of their enzymatic degradation. *Experientia* **6**, 201–209 (1950).
36. Sanchez, R. A., Ferris, J. P. & Orgel, L. E. Studies in prebiotic synthesis. IV. Conversion of 4-aminoimidazole-5-carbonitrile derivatives to purines. *J. Mol. Biol.* **38**, 121–128 (1968).
37. Glavin, D. P. et al. in *Primitive Meteorites and Asteroids* (ed. Abreu, N.) 205–271 (Elsevier, 2018).
38. Oba, Y. et al. Nucleobase synthesis in interstellar ices. *Nat. Commun.* **10**, 4413 (2019).
39. Saladino, R. et al. Meteorite-catalyzed syntheses of nucleosides and of other prebiotic compounds from formamide under proton irradiation. *Proc. Natl Acad. Sci. USA* **112**, E2746–E2755 (2015).
40. Coutens, A. et al. The ALMA-PILS survey: first detections of deuterated formamide and deuterated isocyanic acid in the interstellar medium. *Astron. Astrophys.* **590**, L6 (2016).
41. Biver, N. et al. Molecular composition of comet 46P/Wirtanen from millimetre-wave spectroscopy. *Astron. Astrophys.* **648**, A49 (2021).
42. Kebukawa, Y., Asano, S., Tani, A., Yoda, I. & Kobayashi, K. Gamma-ray-induced amino acid formation in aqueous small bodies in the early Solar System. *ACS Cent. Sci.* **8**, 1664–1671 (2022).
43. Abe, S., Yoda, I., Kobayashi, K. & Kebukawa, Y. Gamma-ray-induced synthesis of sugars in meteorite parent bodies. *ACS Earth Space Chem.* **8**, 1737–1744 (2024).
44. Fox, S. W. & Harada, K. Synthesis of uracil under conditions of a thermal model of prebiological chemistry. *Science* **133**, 1923–1924 (1961).
45. Füri, E. & Marty, B. Nitrogen isotope variations in the Solar System. *Nat. Geosci.* **8**, 515–522 (2015).
46. Okazaki, R. et al. Noble gases and nitrogen in samples of asteroid Ryugu record its volatile sources and recent surface evolution. *Science* **379**, abo0431 (2023).
47. Oba, Y., Takano, Y., Dworkin, J. P. & Naraoka, H. Ryugu asteroid sample return provides a natural laboratory for primordial chemical evolution. *Nat. Commun.* **14**, 3107 (2023).

48. Hatakeda, K. et al. Homogeneity and heterogeneity in near-infrared FTIR spectra of Ryugu returned samples. *Earth Planets Space* **75**, 46 (2023).
49. Yoshimura, T. et al. Breunnerite grain and magnesium isotope chemistry reveal cation partitioning during aqueous alteration of asteroid Ryugu. *Nat. Commun.* **15**, 6809 (2024).
50. Sasaki, K. et al. Metabolomics platform with capillary electrophoresis coupled with high-resolution mass spectrometry for plasma analysis. *Anal. Chem.* **91**, 1295–1301 (2019).

## Acknowledgements

We are grateful to all members involved the Hayabusa2 project organized by JAXA, the Hayabusa2 initial analysis team and the Astromaterials Science Research Group in the Institute of Space and Astronautical Science (ISAS), which made the return of samples from asteroid Ryugu possible. We thank the AO3 issued by ISAS/JAXA for allocating the Ryugu A0480 and C0370 aggregate samples to this research project. This study is part of an official collaboration between JAMSTEC, HMT and IAB at Keio University. This work was supported by the Japan Society for the Promotion of Science (KAKENHI Grant Nos. 21J00504 and 25K17463 to T.K., 21KK0062 to Y.T., 21H04501, 21H05414 and 25H00677 to Y.O. and 23H00148 to H.N.). This research was partially supported by a joint project of the Institute of Low Temperature Science, Hokkaido University.

## Author contributions

T.K., Y.O., Y.T. and H.N. outlined the working flow in this study. T.K. and Y.O. conducted the extraction and purification procedure. T.K., Y.O. and H.N. performed the molecular analysis with the LC/Orbitrap system. N.O.O., N.O. and Y.T. provided the series of authentic C and N isotope standards and conducted the analysis of elemental and isotopic compositions. K.S., H.S. and Y.T. conducted the analysis with the CE/Orbitrap system. All authors discussed the results and commented on the paper.

## Competing interests

The authors declare no competing interests.

## Additional information

**Extended data** is available for this paper at https://doi.org/10.1038/s41550-026-02791-z.

**Supplementary information** The online version contains supplementary material available at https://doi.org/10.1038/s41550-026-02791-z.

**Correspondence and requests for materials** should be addressed to Toshiki Koga.

**Peer review information** *Nature Astronomy* thanks Grégoire Danger and Angel Mojarro for their contribution to the peer review of this work. Peer reviewer reports are available.

https://doi.org/10.1038/s41550-026-02791-z

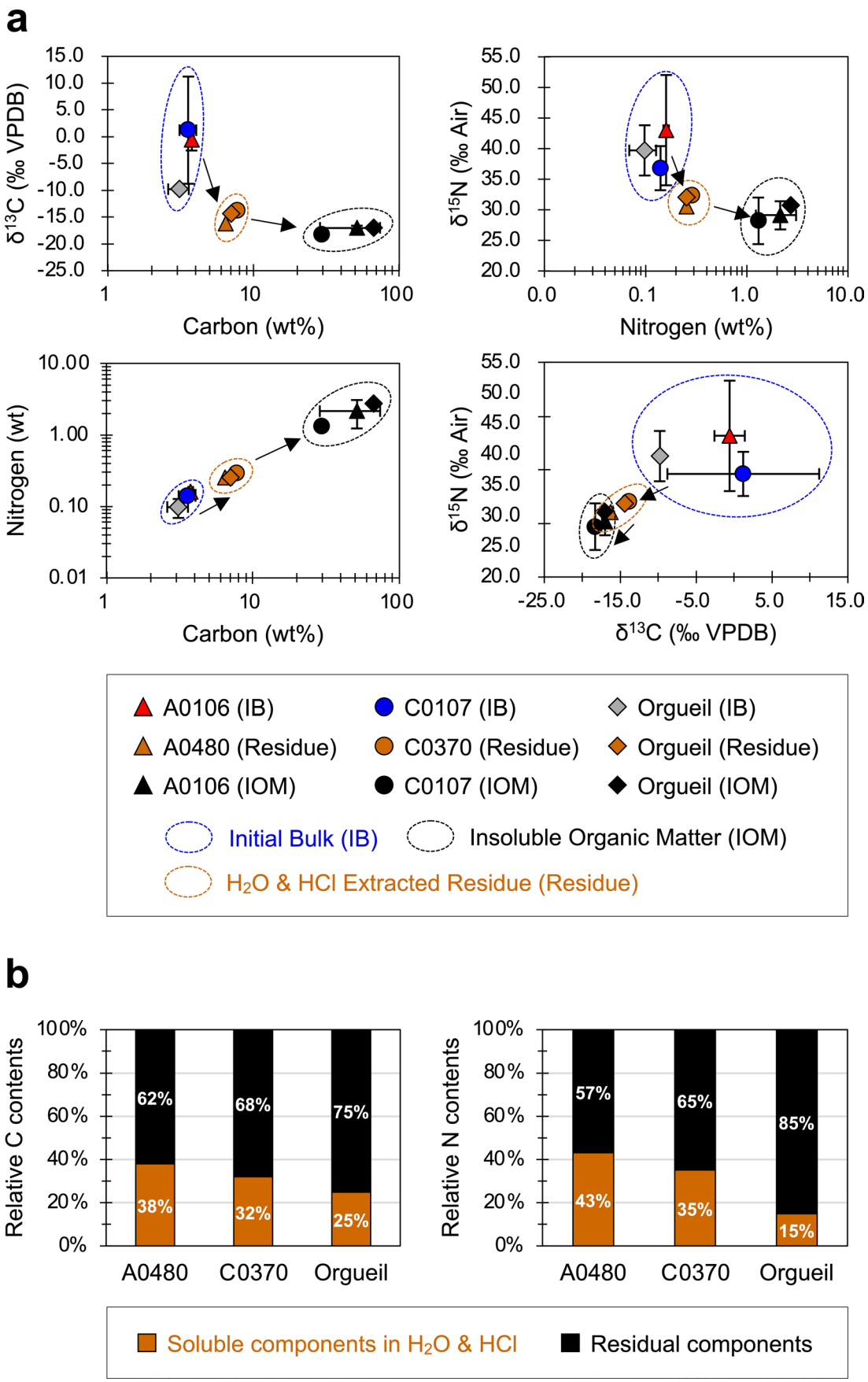


**Extended Data Fig. 1 | See next page for caption.**

https://doi.org/10.1038/s41550-026-02791-z

**Extended Data Fig. 1 | Carbon and nitrogen isotope compositions of the extracted residues from the Ryugu and Orgueil samples. a**, Carbon and nitrogen contents (wt%) and isotopic shifts observed in the residues extracted with $H_2O$ and HCl (Residue), analyzed by nano-EA/IRMS (Extended Data Table 1). Data for the initial bulk (IB) and insoluble organic matter (IOM) of the asteroid Ryugu and Orgueil meteorite were compiled from previous references[17,21,26,33], with IB in red (Ryugu A0106), blue (Ryugu C0107), and gray (Orgueil), residues in brown, and all IOM in black. The carbon and nitrogen contents in the Residue and IOM increased due to the dissolution of silicates and other mineral phases. **b**, Estimated relative carbon and nitrogen contents in the soluble components in $H_2O$ and HCl extracts (brown) and the residual components (black) (Extended Data Table 1).

https://doi.org/10.1038/s41550-026-02791-z

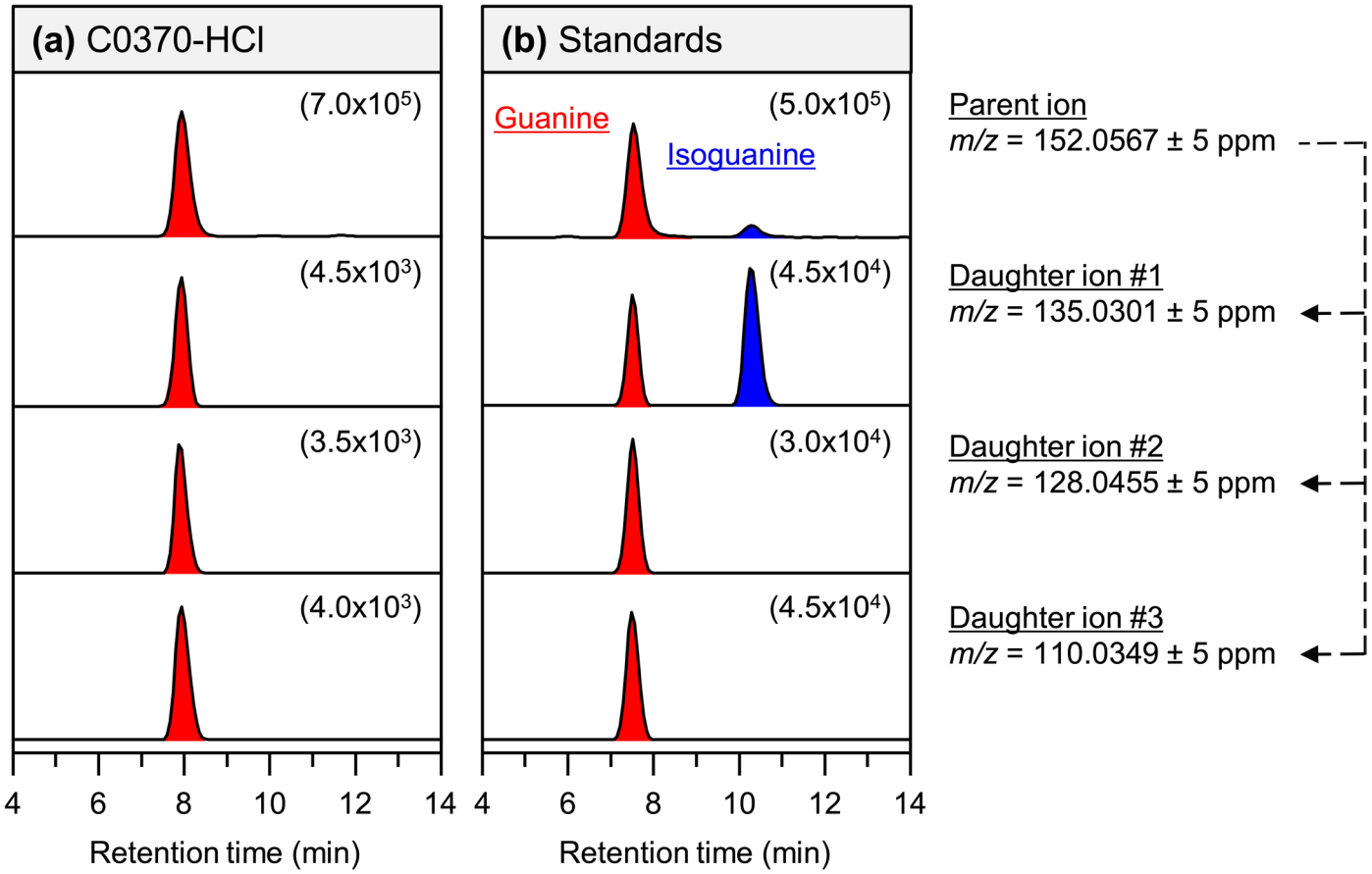


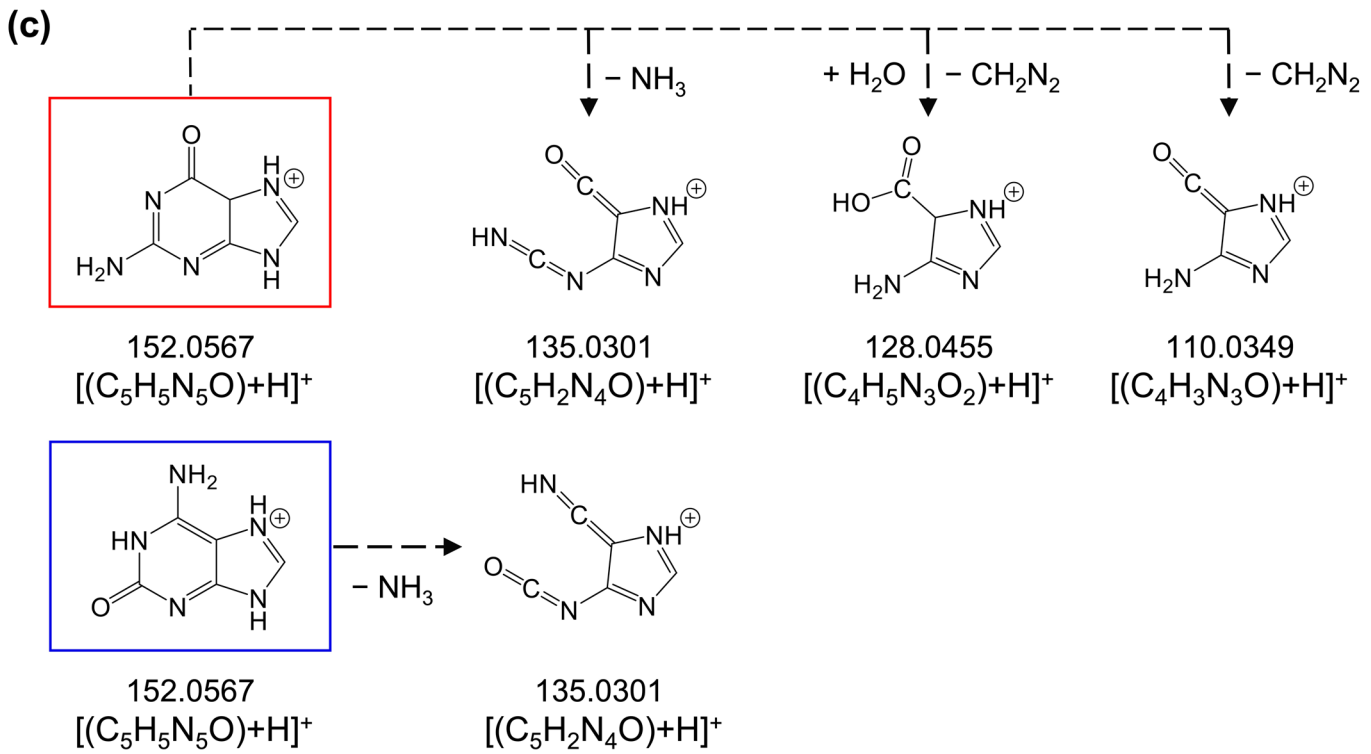


**Extended Data Fig. 2 | The identification of guanine in the Ryugu C0370 sample by MS/MS experiments.** Mass chromatograms at the *m/z* of 152.0567, 135.0301, 128.0455, and 110.0349, corresponding to precursor and product ions of guanine (red) and isoguanine (blue) observed by MS/MS experiments, for (**a**) the C0370-HCl extract and (**b**) guanine (140 femto-mol) and isoguanine (15 femto-mol) standard reagents. Numbers in parentheses indicate the vertical axis range in each chromatogram. (**c**) Proposed fragmentation patterns of guanine and isoguanine measured in MS/MS experiments.

https://doi.org/10.1038/s41550-026-02791-z

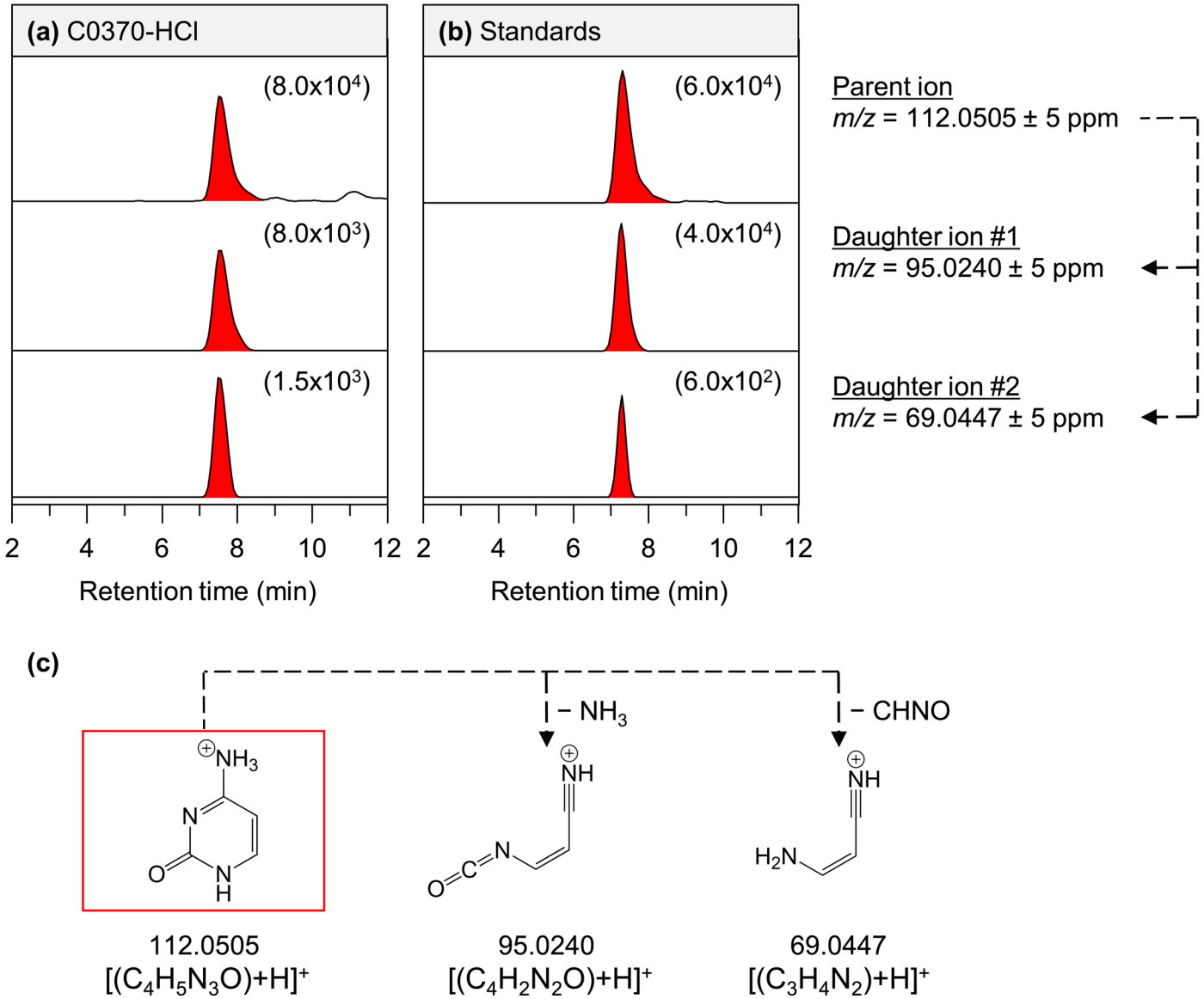


**Extended Data Fig. 3 | The identification of cytosine in the Ryugu C0370 sample by MS/MS experiments.** Mass chromatograms at the m/z of 113.0346, 95.0240, and 69.0447, corresponding to precursor and product ions of cytosine (red) observed by MS/MS experiments, for (**a**) the C0370-HCl extract and (**b**) cytosine standard reagent (100 femto-mol). Numbers in parentheses indicate the vertical axis range of each chromatogram. (**c**) Proposed fragmentation patterns of cytosine measured in MS/MS experiments.

https://doi.org/10.1038/s41550-026-02791-z

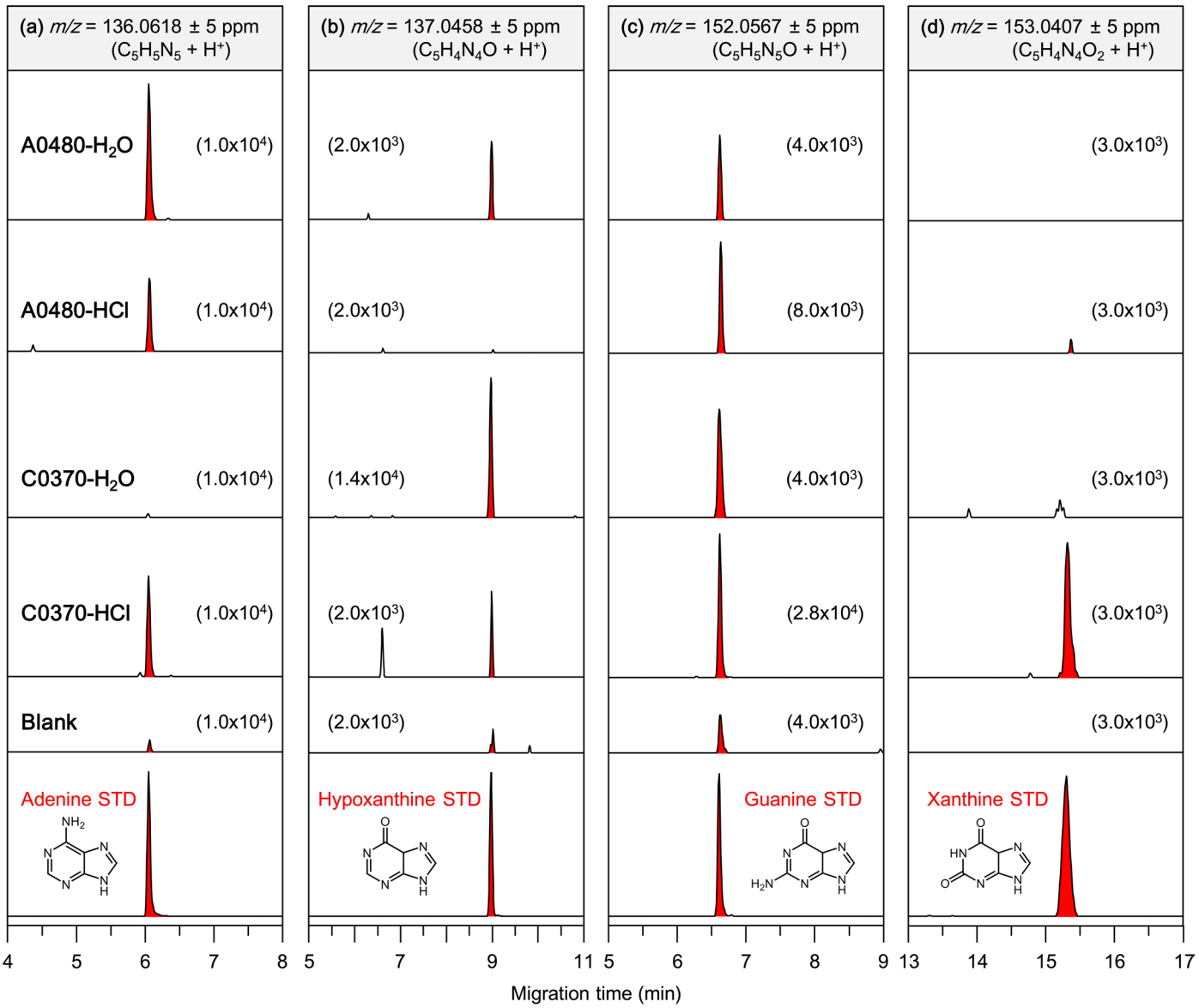


**Extended Data Fig. 4 | Purine nucleobases detected in the $H_2O$ and HCl extracts of Ryugu A0480 and C0370 samples using CE-HRMS analysis.** Mass chromatograms at the *m/z* of (**a**) 136.0618, (**b**) 137.0458, (**c**) 152.0567, and (**d**) 153.0407, corresponding to the protonated molecular ions of adenine ($C_5H_5N_5$), hypoxanthine ($C_5H_4N_4O$), guanine ($C_5H_5N_5O$), and xanthine ($C_5H_4N_4O_2$), respectively. Data for the procedural blank sample and authentic standards are also shown for comparison. Nucleobases identified with standards are shown in red. Numbers in parentheses indicate the vertical axis range in each sample chromatogram.

https://doi.org/10.1038/s41550-026-02791-z

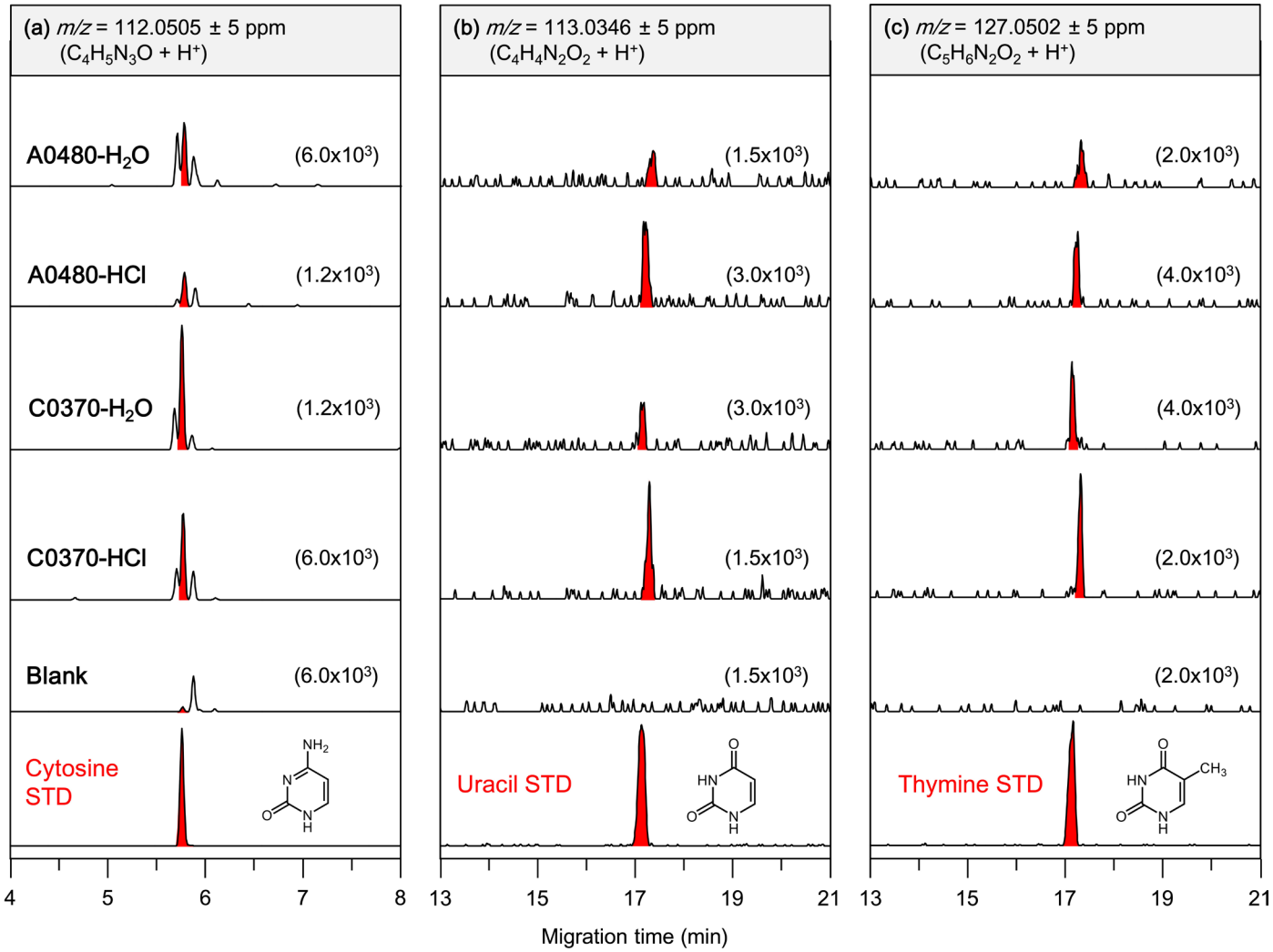


**Extended Data Fig. 5 | Pyrimidine nucleobases detected in the $H_2O$ and HCl extracts of the Ryugu A0480 and C0370 samples using CE-HRMS analysis.** Mass chromatograms at *m/z* values of (**a**) 112.0505, (**b**) 113.0346, and (**c**) 127.0502, corresponding to the protonated molecular ions of cytosine ($C_4H_5N_3O$), uracil ($C_4H_4N_2O_2$), and thymine ($C_5H_6N_2O_2$), respectively. Data for the procedural blank sample and authentic standards are also shown for comparison. Nucleobases identified with standards are shown in red. Numbers in parentheses indicate the vertical axis range in each sample chromatogram.

https://doi.org/10.1038/s41550-026-02791-z

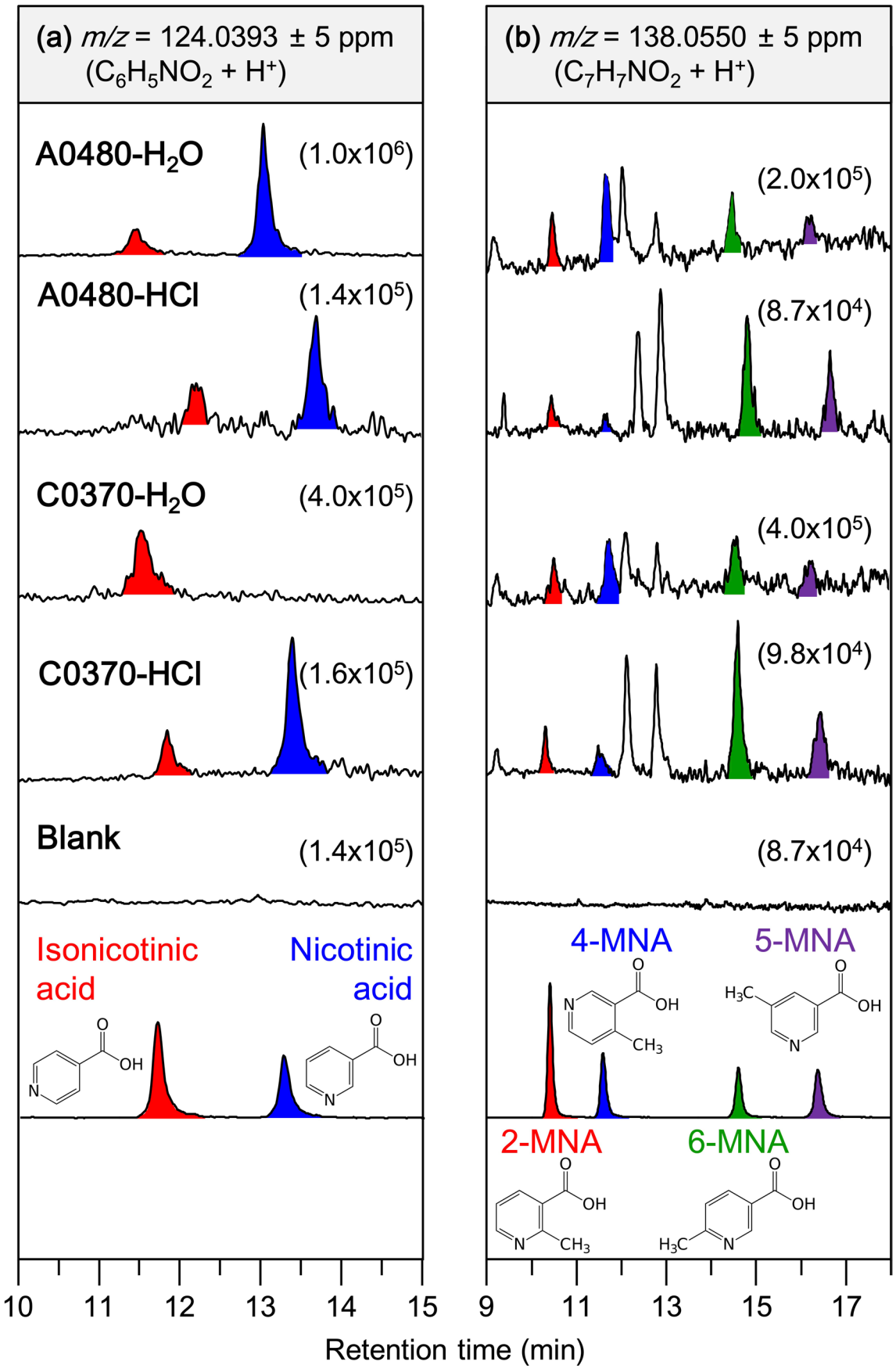


**Extended Data Fig. 6 | See next page for caption.**

https://doi.org/10.1038/s41550-026-02791-z

**Extended Data Fig. 6 | Nicotinic acid and its relevant molecules detected in the HCl extracts of Ryugu A0480 and C0370 samples using HPLC/ESI-HRMS analysis.** Mass chromatograms at *m/z* values of (**a**) 124.0393 and (**b**) 138.0550, corresponding to the protonated molecular ions of nicotinic acid and isonicotinic acid ($C_6H_5NO_2$), and 2-methylnicotinic acid (2-MNA), 4-methylnicotinic acid (5-MNA), 5-methylnicotinic acid (5-MNA), and 6-methylnicotinic acid (6-MNA) ($C_7H_7NO_2$), respectively. Data for the procedural blank sample and authentic standards are also shown for comparison. N-heterocycles identified with standards are shown in red, blue, green, and purple. Numbers in parentheses indicate the vertical axis range in each sample chromatogram.

https://doi.org/10.1038/s41550-026-02791-z

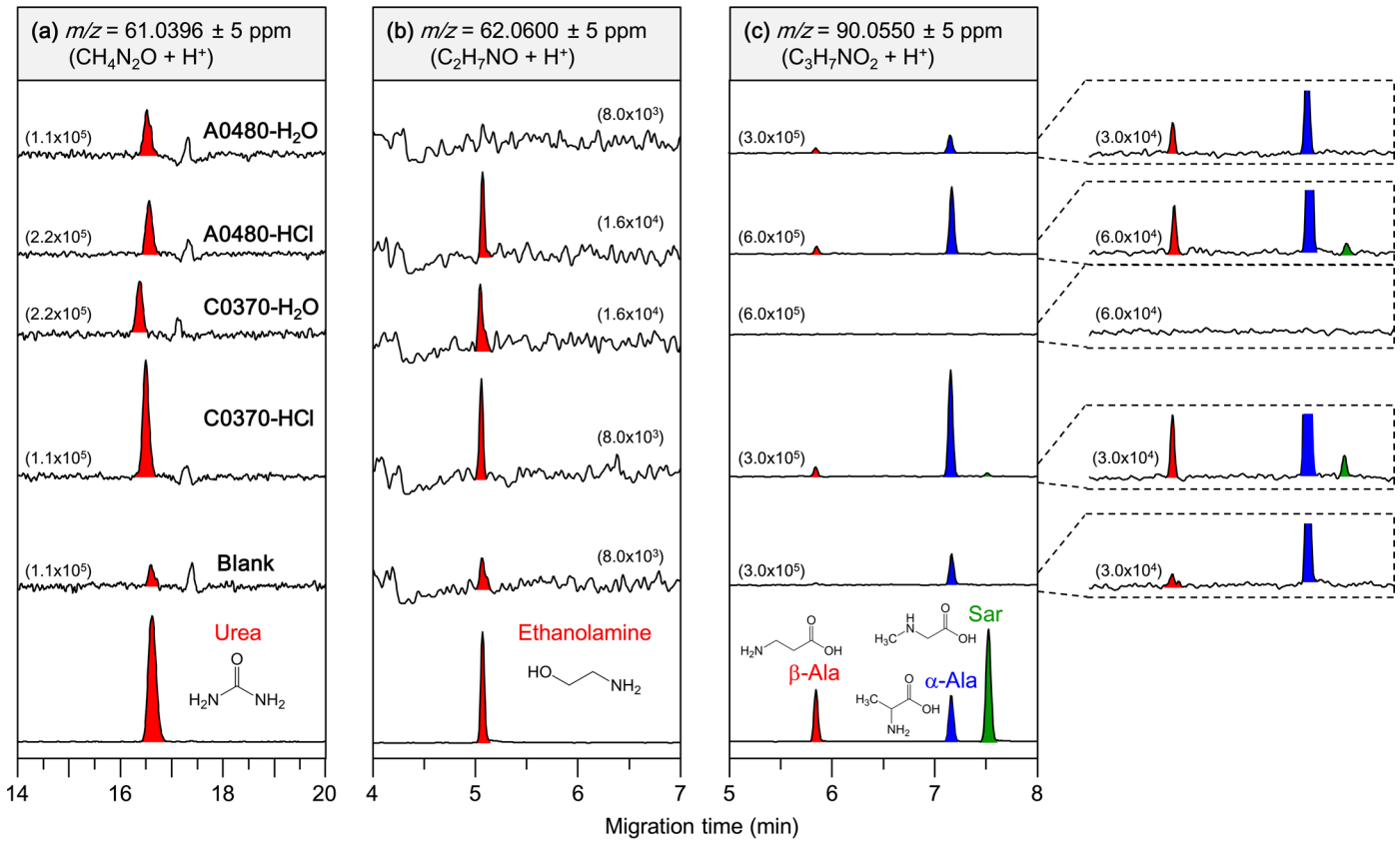


**Extended Data Fig. 7 | N-containing molecules detected in the $H_2O$ and HCl extracts of Ryugu A0480 and C0370 samples using CE-HRMS analysis.** Mass chromatograms at *m/z* values of (**a**) 61.0396, (**b**) 62.0600, and (**c**) 76.0393, corresponding to the protonated molecular ions of urea ($CH_4N_2O$), ethanolamine ($C_2H_7NO$), and $C_3$ amino acids [α-alanine (α-Ala), β-alanine (β-Ala), and sarcosine (Sar) ($C_3H_7NO_2$)], respectively. The chromatograms for $C_3$ amino acids were enlarged to facilitate clearer visualization of the detection of β-alanine and sarcosine. Data for the procedural blank sample and authentic standards are also shown for comparison. N-containing molecules identified with standards are shown in red, blue, and green. Numbers in parentheses indicate the vertical axis range in each sample chromatogram.

https://doi.org/10.1038/s41550-026-02791-z

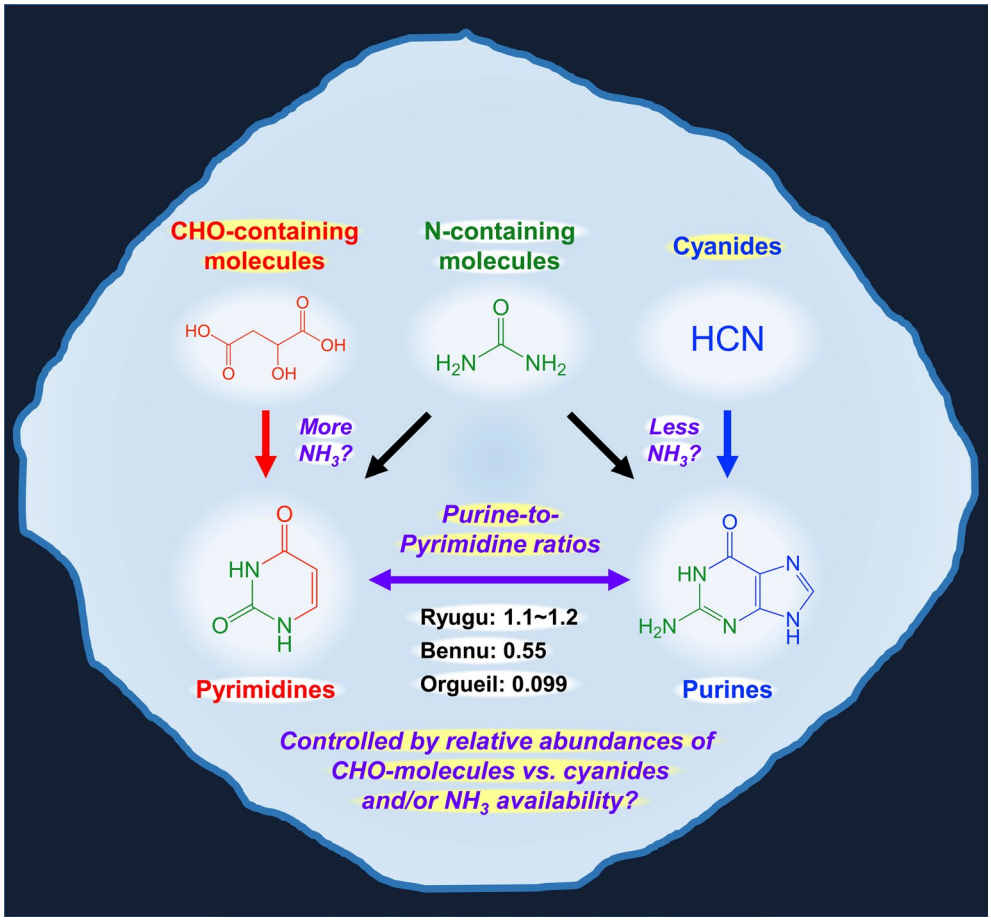


**Extended Data Fig. 8 | Conceptual view of nucleobase synthetic pathways occurred in parent bodies of Ryugu, Bennu, and Orgueil.** A conceptual schematic illustrating how relative abundances of CHO-containing molecules (for example, malic acid), N-containing molecules (for example, urea), and cyanides (for example, HCN), together with the availability of $NH_3$, may influence purine-to-pyrimidine (Pu/Py) production ratios in carbonaceous asteroid parent bodies. Higher $NH_3$ availability may favor pyrimidine formation pathways involving CHO-rich precursors, whereas lower $NH_3$ conditions may promote purine formation pathways involving cyanide chemistry. The resulting Pu/Py ratios observed in the Ryugu, Bennu, and Orgueil samples are shown for comparison, illustrating how variations in parent-body chemistry could lead to distinct nucleobase distributions.

https://doi.org/10.1038/s41550-026-02791-z

**Extended Data Table 1 | Summary of the data obtained for carbon and nitrogen (wt %) with their stable isotopic compositions for the initial bulk, extracted residues, and IOM of the Ryugu and Orgueil**

| Sample weights | Ryugu A0480 | Ryugu C0370 | Orgueil |
|---|---|---|---|
| | this study | this study | this study |
| Initial sample weight (mg) | 11.9 | 8.3 | 30.6 |
| Residual sample weight after $H_2O$ and HCl extraction (mg) | 4.3 | 2.6 | 10.1 |
| Ratio (Residual/Initial) | 36% | 31% | 33% |

| Residue compositions | Ryugu A0480 | Ryugu C0370 | Orgueil |
|---|---|---|---|
| | this study | this study | this study |
| Carbon (wt%) | 6.44 | 7.80 | 7.04 |
| $\delta^{13}C$ (‰ vs. VPDB) | −16.3 | −13.8 | −14.4 |
| Nitrogen (wt%) | 0.25 | 0.29 | 0.25 |
| $\delta^{15}N$ (‰ vs.Air) | +30.5 | +32.3 | +32.0 |
| weight C/N ratio | 25.6 | 27.0 | 27.7 |

| Bulk compositions | Ryugu A0106 | Ryugu C0107 | Orgueil |
|---|---|---|---|
| | Naraoka et al.[17] | Oba et al.[26] | Naraoka et al.[17] and references therein |
| Carbon (wt%) | 3.76 ± 0.14 | 3.58 ± 0.47 | 3.10 ± 0.50 |
| $\delta^{13}C$ (‰ vs. VPDB) | −0.58 ± 2.0 | +1.22 ± 10.0 | −9.8 ± 0.2 |
| Nitrogen (wt%) | 0.16 ± 0.01 | 0.14 ± 0.01 | 0.098 ± 0.029 |
| $\delta^{15}N$ (‰ vs.Air) | +43.0 ± 9.0 | +36.8 ± 3.6 | +39.7 ± 4.1 |
| weight C/N ratio | 23.5 ± 0.4 | 26.0 ± 2.4 | 31.6 ± 5.1* |

| IOM compositions | Ryugu A0106 | Ryugu C0107 | Orgueil |
|---|---|---|---|
| | Takano et al.[21] | Takano et al.[21] | Alexander et al.[33] |
| Carbon (wt%) | 51.2 ± 22.6 | 29.5 ± 2.0 | 67.0 ± 0.7 |
| $\delta^{13}C$ (‰ vs. VPDB) | −17.0 ± 0.4 | −18.3 ± 0.6 | −17.05 ± 0.04 |
| Nitrogen (wt%) | 2.15 ± 0.92 | 1.30 ± 0.14 | 2.73* |
| $\delta^{15}N$ (‰ vs.Air) | +29.1 ± 2.3 | +28.2 ± 3.8 | +30.7 ± 0.2 |
| weight C/N ratio | 23.6 ± 0.8 | 22.6 ± 1.4 | 24.6* |

| Estimated soluble components into $H_2O$ and HCl | Ryugu A0480 | Ryugu C0370 | Orgueil |
|---|---|---|---|
| | this study | this study | this study |
| Carbon (wt%) | 2.22 | 1.65 | 1.17 |
| $\delta^{13}C$ (‰ vs. VPDB) | +25.5 | +33.9 | +3.7 |
| Nitrogen (wt%) | 0.11 | 0.07 | 0.02 |
| $\delta^{15}N$ (‰ vs.Air) | +59.8 | +45.1 | +83.7 |
| weight C/N ratio | 20.7 | 22.9 | 53.9 |
| Carbon (wt%) in soluble:residual | 38:62 | 32:68 | 25:75 |
| Nitrogen (wt%) in soluble:residual | 43:57 | 35:65 | 15:85 |

The residue samples in this study were analyzed only once due to the limited sample amounts. The analytical errors for carbon (wt%), $\delta^{13}C$ (‰ vs. VPDB), nitrogen (wt%), and $\delta^{15}N$ (‰ vs. Air), determined from repeated measurements of working standards, were ± 0.30, ± 0.27, ± 0.037, and ± 0.50, respectively (1σ).

https://doi.org/10.1038/s41550-026-02791-z

**Extended Data Table 2 | Blank-subtracted abundances (in nmol $g^{-1}$) of N-containing molecules detected in the Ryugu A0480 and C0370 samples using CE-HRMS**

| Abundances | A0480 | | | C0370 | | |
|---|---|---|---|---|---|---|
| (nmol $g^{-1}$) | $H_2O$ | HCl | Total | $H_2O$ | HCl | Total |
| ***Amino acids*** | | | | | | |
| DL-α-Alanine | n.q. | 5.5 | 5.5 | n.d. | 7.4 | 7.4 |
| β-Alanine | 0.37 | 0.93 | 1.3 | n.d. | 0.85 | 0.85 |
| Sarcosine | n.d. | 0.27 | 0.27 | n.d. | 0.33 | 0.33 |
| ***Other N-containing molecules*** | | | | | | |
| Urea | 10 | 40 | 50 | 75 | 57 | 132 |
| Ethanolamine | n.d. | 0.083 | 0.083 | 0.21 | 0.067 | 0.28 |

n.d. = not detected (below the detection of limit)
n.q. = not quantified (below the procedural blank)

Water (25°C for 15 min; in triplicate) and HCl extracts (110°C for 12 h) of the Ryugu aggregate samples (A0480, 11.9 mg; C0370, 8.3 mg) were analyzed. Compounds were identified using authentic standards. The reported abundances are based on single-run measurements.